SEMIMAGNETIC SEMICONDUCTORS

Robert R. GAŁĄZKA

Institute of Physics, Polish Academy of Sciences,
Al. Lotników 32/46 02-668 Warsaw, Poland

1. Introduction, General Remarks

Semimagnetic semiconductors (SMS) are a group of solids at the interface between semiconductors and magnetic materials. Semimagnetic semiconductors (also referred to as diluted magnetic semiconductors) are semiconductor-based solid solutions where a part of the cations are replaced by transition metals or rare earth elements. The crystallographic structure of the semiconductor is conserved; the lattice constant is a function of composition. From a magnetic point of view SMS is a disordered magnetic material, since magnetic atoms are randomly distributed in cation sublattice of the semiconductor compound. Table 1 presents the most complete list of bulk ternary SMS. Quaternary SMS are also investigated (e.g., PbSnMnTe or CdMnSeTe). The table does not contain III-V SMS obtained by MBE technique, although these broadly investigated materials can be treated as 3D bulk crystals. The table contains only crystals obtained under thermodynamic equilibrium conditions, whilst III-V SMS and some other SMS obtained by MBE are rather metastable structures.

Generally speaking, in SMS there coexist two interrelated and interacting subsystems: mobile delocalized charge carriers and localized magnetic moments connected with paramagnetic ions. Electronic properties of SMS have been the subject of intensive studies since early seventies. Due to the strong spin exchange interaction between mobile carriers and localized magnetic moments (the exchange constant of the sp-d interaction is of the order of 1 eV for II-VI SMS), significant changes of the band structure and behavior of carriers were observed. A number of new physical phenomena were discovered, such as giant Faraday rotation, the magnetic field induced metal-insulator transition, the bound magnetic polaron, the quantum thermomagnetic oscillations. Magnetic properties of SMS are the subject of studies since about 1980. Investigations of the influence of electron subsystem on magnetic properties of SMS are connected with the observation of a ferromagnetic phase in PbSnMnTe induced by carrier concentration – 1986, and other more subtle effects as magnetic polaron.

About 10 years later, molecular beam epitaxy (MBE) grown GaAs with Mn opened a new chapter of III-V SMS showing ferromagnetic behavior with the highest transition temperature T_C = 140 K. In 1987, the first paper devoted to layered structure and magnetic properties of low dimensional (LD) SMS was published starting intensive studies of superlattices and other LD structures made of SMS.

Table 1. Composition and crystal structure of ternary bulk SMS: ZB – zinc blende, W – wurtzite, RS – rock salt, RH – rhombohedral. Stars denote SMS with the highest reported *x* value (reprinted from Journal of Magnetism and Magnetic Materials, Vol. 140-144 (1995), R.R. Gałązka, p. 13).

Material	Crystal structure	Composition range
II-VI (Mn)		
$Zn_{1-x}Mn_xS$	ZB	$0 < x \leq 0.10$
	W	$0.10 < x \leq 0.45$
$Zn_{1-x}Mn_xSe$	ZB	$0 < x \leq 0.30$
	W	$0.30 < x \leq 0.57$
$Zn_{1-x}Mn_xTe$	ZB	$0 < x \leq 0.86$
$Cd_{1-x}Mn_xS$	W	$0 < x \leq 0.45$
$Cd_{1-x}Mn_xSe$	W	$0 < x \leq 0.50$
$Cd_{1-x}Mn_xTe$	ZB	$0 < x \leq 0.77$
$Hg_{1-x}Mn_xS$	ZB	$0 < x \leq 0.37$
$Hg_{1-x}Mn_xSe$	ZB	$0 < x \leq 0.38$
$Hg_{1-x}Mn_xTe$	ZB	$0 < x \leq 0.35$
II-V (Mn)		
$(Cd_{1-x}Mn_x)_3As_2$	Tetra.	$0 < x \leq 0.18$
$(Zn_{1-x}Mn_x)_3As_2$	tetr.	$0 < x \leq 0.15$
IV-VI (Mn, Eu, Gd)		
$Pb_{1-x}Mn_xS$	RS	$0 < x \leq 0.05$
$Pb_{1-x}Mn_xSe$	RS	$0 < x \leq 0.17$
$Pb_{1-x}Mn_xTe$	RS	$0 < x \leq 0.12$
$Sn_{1-x}Mn_xTE$	RS	$0 < x \leq 0.40$
$Ge_{1-x}Mn_xTe$	RH	$0 < x \leq 0.18$
	RS	$0.18 < x \leq 0.50$
$Pb_{1-x}Eu_xSe$	RS	$0 < x \leq 0.04$*
$Pb_{1-x}Eu_xTe$	RS	$0 < x \leq 0.32$*
$Sn_{1-x}Eu_xTe$	RS	$0 < x \leq 0.013$
$Pb_{1-x}Gd_xTe$	RS	$0 < x \leq 0.11$*
$Sn_{1-x}Gd_xTe$	RS	$0 < x \leq 0.09$*
II-VI (Fe, Co, Cr)		
$Zn_{1-x}Fe_xS$	ZB	$0 < x \leq 0.26$*
$Zn_{1-x}Fe_xSe$	ZB	$0 < x \leq 0.22$*

$Zn_{1-x}Fe_xTe$	ZB	$0 < x \le 0.01$*
$Cd_{1-x}Fe_xS$	W	$0 < x < 0.09$*
$Cd_{1-x}Fe_xSe$	ZB	$0 < x < 0.20$
$Cd_{1-x}Fe_xTe$	ZB	$0 < x \le 0.06$*
$Hg_{1-x}Fe_xS$	ZB	$0 < x \le 0.037$*
$Hg_{1-x}Fe_xSe$	ZB	$0 < x \le 0.20$*
$Hg_{1-x}Fe_xTe$	ZB	$0 < x \le 0.02$*
$Zn_{1-x}Co_xS$	ZB	$0 < x \le 0.15$*
$Zn_{1-x}Co_xSe$	ZB	$0 < x \le 0.10$*
$Zn_{1-x}Co_xTe$	ZB	$0 < x < 0.06$*
$Cd_{1-x}Co_xS$	W	$0 < x \le 0.064$*
$Cd_{1-x}Co_xSe$	W	$0 < x \le 0.082$*
$Cd_{1-x}Co_xTe$	ZB	$0 < x \le 0.04$
$Hg_{1-x}Co_xS$	ZB	$0 < x \le 0.02$
$Hg_{1-x}Co_xSe$	ZB	$0 < x \le 0.047$*
$Zn_{1-x}Cr_xSe$	ZB	$0 < x \le 0.005$*
$Zn_{1-x}Cr_xTe$	ZB	$0 < x \le 0.003$*
$Cd_{1-x}Cr_xS$	W	$0 < x \le 0.002$*

2. Energy Band Structure And Semiconductor Properties Of SMS

Replacing cations such as Cd or Hg with a paramagnetic ion such as Mn in the same crystallographic structure does not markedly disturb the semiconductor properties of the material. The energy gap changes (increases) but the conduction and valence bands conserve their symmetry and character as in nonmagnetic semiconductor mixed crystals. The spin momenta of paramagnetic ions are connected with the 3d or 4f shell, for transition metals or rare earth elements, respectively. The energy level of 3d or 4f electrons lies below the top of the valence band and thus has negligible influence on its shape or that of the bottom of the conduction band. Thus, all basic semiconductor properties connected with the band symmetry and topology are the same as for a typical semiconductor and the only influence of the magnetic subsystems on electrons comes from the spin exchange interaction between mobile carriers and localized magnetic ions. This interaction can be represented by a Heisenberg term

$$H_{ex} = \bar{\sigma}\sum \bar{S}_i J\left(\vec{r} - \vec{R}\right) \qquad (1)$$

Where $\bar{\sigma}$ and $\bar{S}$ are spin operators of the band electron and magnetic ion, respectively, the summation is over all lattice sites occupied by the magnetic ions, *J* is the exchange constant.
Assuming mean field and virtual crystal approximations, this term can be rewritten in the form periodic with a lattice constant:

$$H_{ex} = x\bar{S}_{av}\bar{\sigma}\sum_R J\left(\vec{r} - \vec{R}\right) \qquad (2)$$

where x is the molar fraction of magnetic ions, $\langle \bar{S} \rangle_{av}$ is the average over all magnetic ions and is directly related to the magnetization of sample equal:

$$M = N_0 g \mu \langle \bar{S} \rangle_{av} \qquad (3)$$

N_0 is the number of unit cells per unit volume, g – the Lande factor for magnetic ions, μ – the Bohr magneton.

The Heisenberg term must be added to the effective mass Hamiltonian to solve the energy eigenproblem for SMS. Realizing this was the turning point in understanding their properties and provided a basis for this group of alloys to be distinguished from other semiconductor mixed crystals. Since that time SMS has become the subject of intensive studies in Europe and other countries.

Strictly speaking, the Hamiltonian should also contain a term representing the paramagnetic ion-ion exchange interaction and responsible for magnetic properties of SMS.
However, that term is about three orders of magnitude smaller than term (2). For this reason, for energy band structure determination one can neglect the paramagnetic ions interaction term, which also significantly simplifies further calculations.

It is worth to notice that experimentally measured magnetization, which can serve to evaluate $\langle \bar{S} \rangle_{av}$ (eq. 3), reflects all magnetic interactions present in the crystal, thus also the ion-ion exchange interaction is, in fact, included in the band structure determination although not a straight forward way.

The exchange interaction depends on the ion spin and the exchange constant. The spin of Mn is the highest for transition metals and equals 5 Bohr magnetons, and whilst a typical value for the exchange coupling between magnetic ions $J_{d\text{-}d}$ is 10^{-3} eV, the exchange constant for electrons and holes with magnetic ions $J_{sp\text{-}d}$ is about 1 eV in SMS.

The exchange interaction is also strongly temperature and magnetic field dependent. As was said earlier, the macroscopic magnetization of a sample is proportional to the thermodynamic average value of the magnetic ion spin, so to a good approximation we can replace the ion spin operators in the Hamiltonian by their average value, calculated or taken from measurements of the magnetization. From typical magnetic functions we can thus obtain information on the electron behavior.

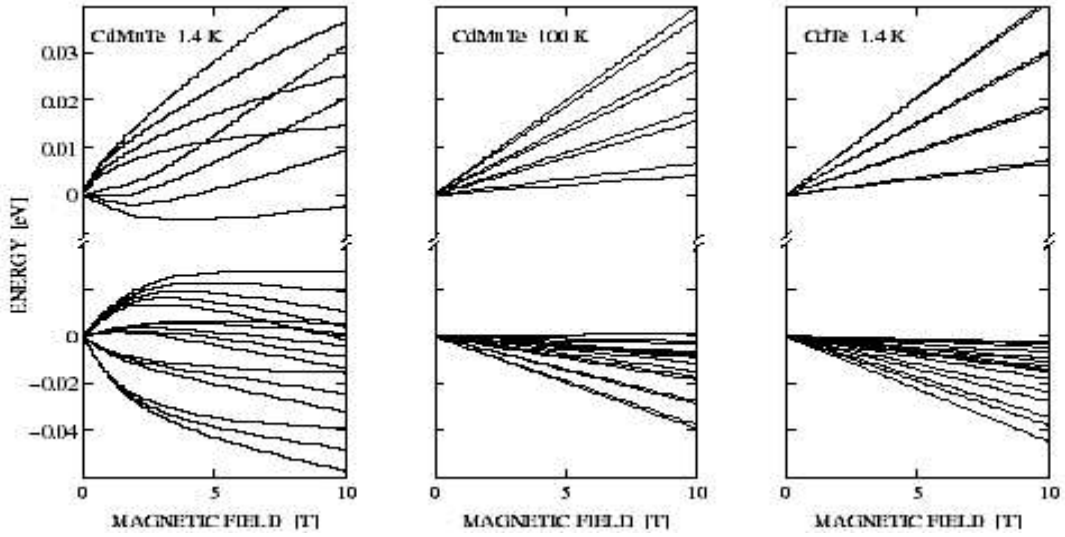

Fig. 1. Conduction and valence bands quantization in external magnetic field of $Cd_{0.95}Mn0_{0.05}Te$ and CdTe. Spin splitting – very weak in CdTe – is the main effect in CdMnTe. Notice the almost equal splitting of the heavy and light hole bands in CdMnTe. The influence of exchange interaction is visible even at 100 K. The picture of CdTe in this range of temperature is practically the same. (After Gałązka R.R. (1987) in: Europhysics News, Vol. 18, p. 90.)

In semiconductors, an external magnetic field acts on both the orbital motion and the spin of electrons producing Landau quantization and spin splitting, to an extent dependent on the effective mass of the carriers. The exchange interaction acts on their spin only and is, in effect, mass independent. Because of this, and also the large value of $J_{sp\text{-}d}$, the band structure in turn changes drastically under the influence of an external magnetic field and depends strongly on temperature.

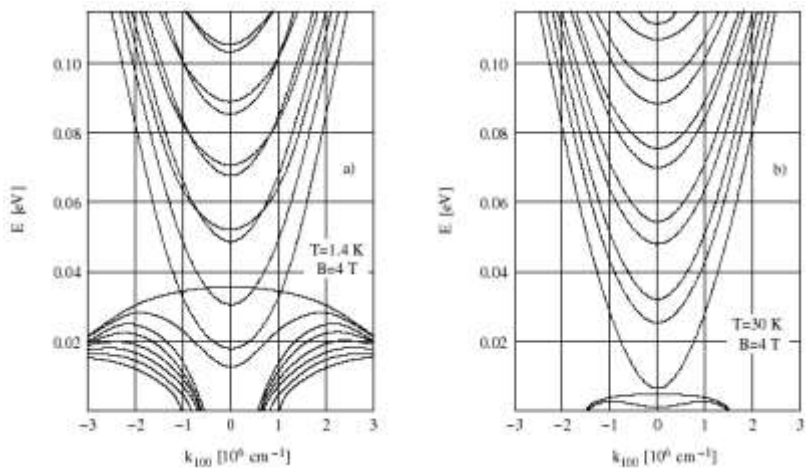

Fig. 2. Energy band structure of $Hg_{1-x}Mn_xTe$, x = 0.02, calculated at 14 K (a) and 30 K (b) in magnetic field H = 4 T (after Gałązka R.R. in: Wilson B.L.M. (ed.) ICPS 14th, Edinburgh Institute of Physics, Conference series no. 43, 1978, p. 133).

From Fig. 1 we can see that the very typical structure of the degeneracy of the light and heavy hole valence bands disappears in SMS when a magnetic field is applied. The change is accompanied by a drastic increase of hole mobility like that observed in low-dimensional structures. In SMS such as $Hg_{1-x}Mn_xTe$ or $Hg_{1-x}Mn_xSe$ (for $x \leq 0.07$), Fig. 2, the magnetic field produces an overlap of the valence and conduction bands, an effect never observed in nonmagnetic semiconductors.

The exchange interaction does not only split the bands but also introduces a substantial band anisotropy.

Calculations of the band structure of SMS have to take into account the symmetry of the crystal, the corresponding form of Hamiltonian and appropriate set of wave functions. In order to illustrate a band structure calculation, let us consider a simpler case than those presented in Figs. 1 and 2. To determine the band structure in the presence of exchange interaction for zinc blende structure with the open energy band gap, one has to take into account the exchange splitting of the Γ_6, Γ_8, and Γ_7 levels when performing the $\vec{k} \cdot \vec{p}$ band calculation. This was done by keeping only terms of the order of k^2 and neglecting the inversion asymmetry and warping, leading to the following results. The splitting of Γ_6 band changes only slowly with $\vec{k}$ and can be described by an effective g-factor. This g-factor is very high and positive even in narrow gap SMS, in spite of the fact that in narrow gap nonmagnetic semiconductors the g-factor of conduction electrons is negative.

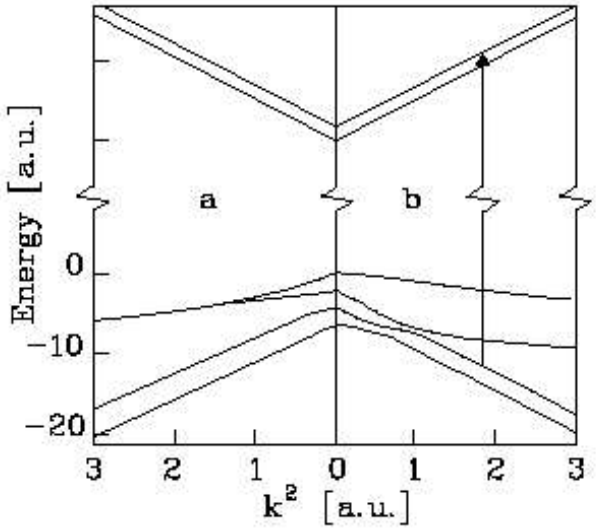

Fig. 3. Splitting of Γ_6 and Γ_8 bands due to the exchange in an open gap semimagnetic semiconductor for two values of angle between $\vec{k}$ and $\vec{B}$: 90° (a) and 10° (b) (after Gaj J.A., Ginter J., and Gałązka R.R. (1978), Physica Status Solidi (b) 89, 655).

For the Γ_8 bands, the splitting depends dramatically on both the direction and the absolute value of $\vec{k}$. This is shown schematically for an open gap band structure in Fig. 3.

The reduced variables used here are $\varepsilon = E/B_{\text{exch}}$, $\vec{\kappa} = \hbar\vec{k}/(2B_{exch}m_{hh})^{1/2}$, where E is the electron energy and m_{hh} is the heavy-hole mass. Of particular interest are the dispersion relations close to the Γ point, i.e., for

$$\hbar^2 k^2 / m_{lh} << |B_{exch}| \qquad (4)$$

B_{exch} is the value connected with H_{exch}, eq. 2, and m_{lh} is the light hole mass. The four non-degenerate valence bands are (the warping of the valence band is neglected)

$$E_{\pm 3/2}(\vec{k}) = 1/2\hbar^2\left[(3/4m_{lh} + 1/4m_{hh})k_\perp^2 + k_z/m_{hh}\right] \pm 3B_{exch} \qquad (5)$$

$$E_{\pm 1/2}(\vec{k}) = 1/2\hbar^2\left[(1/4m_{lh} + 3/4m_{hh})k_\perp^2 + k_z/m_{lh}\right] \pm B_{exch} \qquad (6)$$

Where $\vec{k}_\perp$ is the wave-vector component perpendicular to the magnetic field. Thus, the constant energy surfaces are rotational ellipsoids, cucumber-like for the highest and the lowest bands (±3/2) and disc-like for the intermediate bands (±1/2). For $m_{\text{hh}} >> m_{\text{lh}}$, the mass anisotropy is particularly strong for the bands ±3/2, being equal to $3m_{\text{hh}}/4m_{\text{lh}}$. As $J_{\text{p-d}} > 0$ for known materials, i.e., $B_{\text{exch}} < 0$, $E_{-3/2}(\vec{k})$ is the highest valence band.

For $\vec{k}$ not fulfilling (4), there is a substantial mixing of the wave functions and the dependence of energy on $\vec{k}$ is more complicated.

So far, we have neglected the direct effect of the external magnetic field on the orbital motion of the carrier, as well as the intrinsic spin splitting, taking into account only the ordering of manganese spins by the field and the exchange interaction of carriers with these spins. The direct effect may be neglected, in fact, at rather weak magnetic fields in wide gap SMS, like $Cd_{1-x}Mn_xTe$, because of high effective masses of the carriers (i.e., small Landau splittings) and low g-factors.

In a narrow or zero gap SMS, like $Hg_{1-x}Mn_xTe$, one cannot neglected the direct effect of the external magnetic field on the spin splitting and the orbital motion of the valence electron, as the low effective masses yield high cyclotron frequencies, and *g*-factors are high. The exchange splitting has to be treated together with Landau and Zeeman splittings. This is done by adding the diagonal part of the exchange interaction to the Pidgeon-Brown $\vec{k} \cdot \vec{p}$ Hamiltonian of zinc-blende type semiconductors in a magnetic field. In this Hamiltonian the levels Γ_6, Γ_8, and Γ_7 are treated exactly, and the effects of more distant levels up to the order of k^2. Inversion asymmetry and warping are then neglected. The numerical solution (see Figs. 1, 2) of the modified Pidgeon-Brown Hamiltonian fits very well the positions of the Landau levels in narrow and zero gap $Hg_{1-x}Mn_xTe$, observed in magneto-absorption and magnetotransport measurements.

Impurity levels are also influenced by exchange interactions: the ionization energy of an acceptor decreases and its wave function becomes anisotropic under the influence of a magnetic field. Both effects produce a giant negative magnetoresistance and a field-induced insulator-metal transition. Indeed all the properties susceptible of being changed by a magnetic field are very different in SMS in comparison with ordinary semiconductor – the Faraday effect, Shubnikov-de Haas oscillations, magneto-optical properties, luminescence; these are all different and are also strongly temperature and magnetic field dependent.

In the absence of a magnetic field, the average value of the ion spins is zero, the magnetization is zero too, and SMS should behave as typical nonmagnetic semiconductors. Whereas this is true for delocalized band electrons, when an electron is localized around an impurity, a bound magnetic polaron can be observed. This concept was first introduced to explain the behavior of magnetic semiconductors (Eu chalcogenides) and then later was applied also to SMS. A localized electron can produce a spontaneous magnetization within the range of its wave function via the exchange interaction. Local ferromagnetic ordering in that range produces a Stoke's shift in spin-flip Raman scattering even in the absence of an external magnetic field and other related phenomena. Local fluctuations of magnetization and a detailed knowledge of electronic states are essential for a theoretical description of this effect. The bound magnetic polaron is a subtle example of the feedback between electronic and magnetic subsystems present in SMS.

3. Magnetic Properties

Magnetic properties of SMS connected with the exchange interaction between paramagnetic ions are similar to those of other dilute magnetic materials. The broad range of possible magnetic ion concentrations (up to x=0.80 in $Zn_{1-x}Mn_xTe$ and x =0.70 for $Cd_{1-x}Mn_xTe$) allows us to observe the evolution of magnetic interactions in the same crystallographic structure as a function of magnetic ion concentration. A continuous transition from diamagnetic behavior (for $x \leq 0.005$) of the host semiconductor, to paramagnetism, spin-glass (for $x \geq 0.02$), and finally antiferromagnetic order has been observed. Type III antiferromagnetic ordering is observed for $x > 0.6$ indicating that the magnetic elementary cell contains two elementary cells of the cation sublattice. From a crystallographic point of view the magnetic subsystem is disordered; the distribution of magnetic atoms on the cation sublattice is random.

A spin-glass-like state is observed in SMS in the broadest range of paramagnetic ion concentrations ($0.02 \leq x \leq 0.60$) below and above the percolation threshold, Fig. 4. Indeed the temperature dependence of the magnetic susceptibility below and above the transition temperature and their dynamic properties at low and high magnetic fields suggest rather the existence of two spin-glass phases arising from the competition between spin-glass and clustering behavior. Below the

percolation threshold ($x \leq 0.17$ for fcc lattice) the mechanism responsible for a spin-glass phase is even less clear, although, for such a dilute system it must be long-range to produce freezing of the spins.

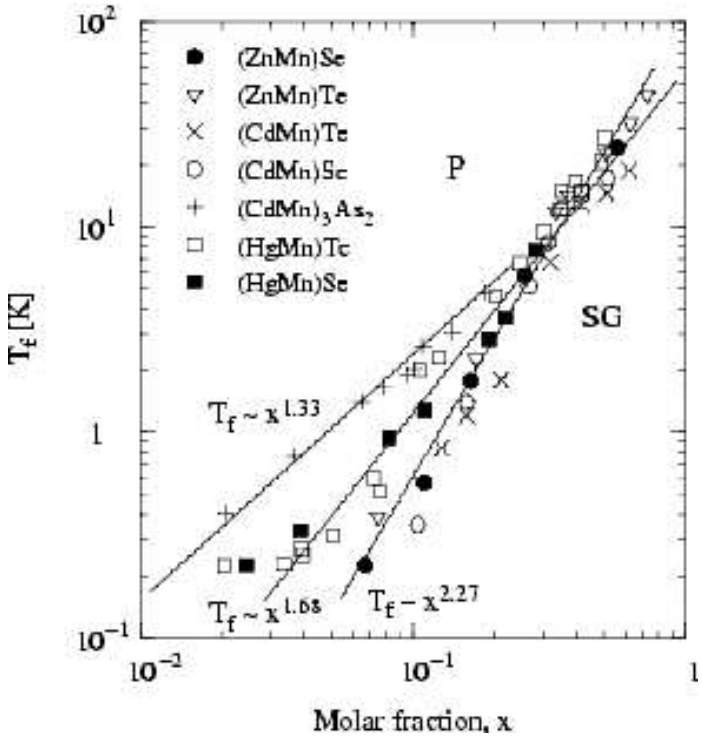

Fig. 4. Magnetic phase diagram for the listed SMS. P – indicates paramagnetic region, SG – indicates the spin-glass region. (After Gałązka R.R. (1995) in: Journal of Magnetism and Magnetic Materials, Vol. 140-144, p. 14.)

The antiferromagnetic order has been inferred from specific heat and magnetic susceptibility measurements, and additional information concerning this phase has come from neutron diffraction studies: only a certain fraction of the total number of magnetic ions (e.g., about 50% for CdMnTe, $x = 0.65$) is well ordered, the rest remain in a disordered spin-glass phase. Thus a mixed phase (antiferromagnetic and spin-glass coexisting together) rather than a truly antiferromagnetic phase is observed.

Despite the variety of semiconductor host compounds, many of magnetic properties are common to the whole group of SMS:
Magnetic phase diagrams are very similar;
Interaction between paramagnetic ions is antiferromagnetic for nearest neighbors;
Both short-range and long-range magnetic interactions are present and are important;
Different magnetic phases coexist.

The influence of basic electronic properties, such as band structure and carrier concentration, on the magnetic properties of SMS is also significant. The former is related to the position of the 3d level of the paramagnetic ion with respect to the valence or conduction bands and on the hybridization of this level. Strong hybridization occurs whenever the 3d level is close to a band extremum provided the symmetry of the band allows the interaction. Moreover, the effective exchange constant $J_{d\text{-}d}$ which is proportional to V_h^4, where V_h is the hybridization energy, also increases. Higher values of $J_{d\text{-}d}$ are observed for sulphides and selenides than for tellurides alloys if the same cation is considered. This is in agreement with the expected upward shift of the 3d level of

Mn, from about 3 eV below the top of the valence band for tellurides, to an energy difference close to zero for sulphides.

The next effect related to the band structure and particularly to the energy gap is the Bloembergen-Rowland mechanism leading to the exponential decay of $J_{d\text{-}d} \sim J_0(-\alpha R)$ for finite gap materials and to a power law decay of $J_{d\text{-}d}$ for zero gap SMS such as HgMnTe or HgMnSe. The exponential or power decay produces a long-range interaction with respect to short-range delta-like interactions usually assumed for exchange mechanisms between magnetic ions. The spin-glass transition temperature is particularly sensitive to the long-range part of the exchange interactions as can be seen in Fig. 4 which gives data on both wide gap SMS and narrow or zero gap HgMnTe and HgMnSe. The difference in the response to changing Mn concentration in the zero or narrow gap SMS suggests that band structure influences spin-glass formation.

4. Ferromagnetic SMS

The influence of carrier concentration on magnetic properties has been extensively investigated in metallic alloys. Several IV-VI semiconductors like SnTe can exhibit quite high metallic-like carrier concentrations. In the quaternary alloy PbSnMnTe, the concentration of holes can be varied by annealing in the range 10^{20} to 5×10^{21} cm^{-3}. In $Pb_{0.25}Sn_{0.72}Mn_{0.03}Te$ an abrupt transition from paramagnetic to ferromagnetic phase has been found for $p > 3\times10^{20}$ cm^{-3}. The Curie temperature is a function of hole concentration, but the Mn ions conserve their magnetic moment of 5 Bohr magnetons. The magnetic phase diagram for this first ferromagnetic SMS, Fig. 5, is thus three dimensional (T, x, n) in contrast to the two-dimensional diagram (T, x) usually presented for magnetic alloys. Even a low concentration of spin polarized carriers when optically pumped can change the magnetization of HgMnTe owing to the strong exchange interaction of carriers with magnetic ions.

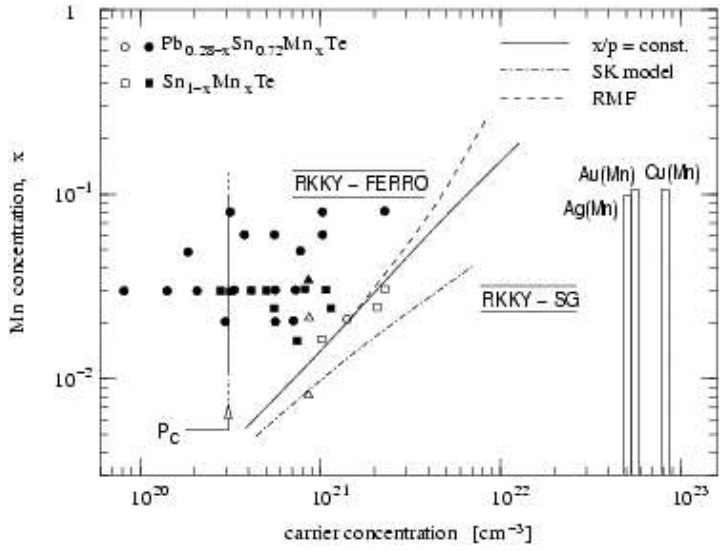

Fig. 5. Magnetic phase diagram for PbSnMnTe (•) and SnMnTe (▪). The ferromagnetic phase is observed in the region above the critical carrier concentration p_c and the straight line defined by the equation x/p = const. Off that region a spin-glass state is observed. Calculated phase boundaries between the ferromagnetic and spin-glass state are also shown for two theoretical models: SK – Sherrington-Kirkpatrick model and RMF – random mean field model. Canonical metallic spin-glasses are also shown. (After de Jonge W.J.M. *et al*. (1992) In: Europhysics Letters, Vol. 17(7), p. 631.)

The equilibrium solubility of magnetic impurities in III-V semiconductors is too low to observe typical SMS behavior. In 1989, using MBE technique it was possible to obtain non-equilibrium crystal growth of InMnAs and later, in 1996, GaMnAs. In both materials *p*-type samples exhibit a ferromagnetic phase with the highest transition temperature T_C = 140 K for Mn concentration x = 0.053 in GaMnAs. Ferromagnetism of these materials is related to the high hole concentration and large exchange constant $J_{p\text{-}d} \approx 1.2$ eV.

Strong p-d exchange interaction is also expected for *p*-type wide gap SMS such as GaMnN or ZnMnO resulting from the small lattice constant, the large effective mass; the position of 3d shell and the small spin-orbit interaction. Some theoretical estimations predict in these materials T_C above room temperature (Fig. 6). In II-VI SMS highly doped for *p*-type, a ferromagnetic behavior, in low temperatures, was also observed (ZnMnTe, modulation doped CdMnTe). The theory of ferromagnetic transition in III-V and II-VI SMS is still not complete, a number of the important questions remain open.

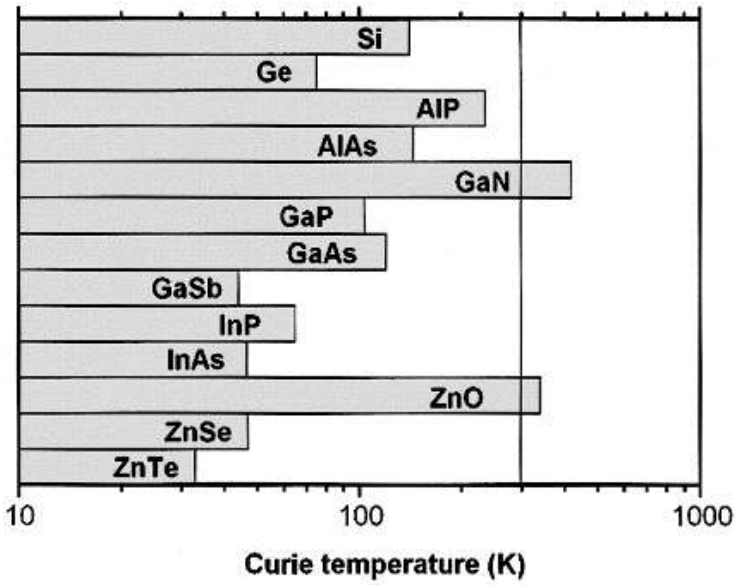

Fig. 6. Computed values of the Curie temperature T_C for various *p*-type semiconductors containing 5% of Mn per cation (2.5% per atom) and 3.5×10^{20} holes per cm^3 (after Dietl T., Ohno H., Matsukura F., Cibert J., Ferrand D. (2000) Science, Vol. 287, p. 1019).

5. Low Dimensional (LD) SMS

Modern technology such as MBE makes it possible to obtain quasi-3D SMS in the whole range of x from 0 to 1. It also gives broad possibilities to create different combinations of semiconductor, SMS, and magnetic materials. From the other side, the dimensionality of LD structures influences the properties of both electronic and magnetic subsystems. Additionally, almost always existing strains also influence the properties of superlattices and other LD structures. Studies of LD SMS not only extend the material base but open a new area of dimension-dependent phenomena and interactions in SMS systems. Among many effects observed in LD SMS structures, we will mention only a few phenomena, where exchange interaction is essential and which cannot be

observed in nonmagnetic LD semiconductors. In all cases giant Zeeman splitting caused by the exchange interaction plays an important role.

In superlattices made of ZnSe/ZnMnSe with a small amount of Mn, band offset of conduction and valence bands is negligible if the magnetic field equals zero. In the presence of an external field the conduction and valence bands of ZnMnSe split creating a spin-superlattice because the spin-split states allow only one spin configuration. The possibility of the existence of such a spin superlattice was earlier suggested for SMS and later experimentally observed. If the superlattice, quantum well or heterostructure is made of SMS and non-SMS material (e.g., ZnTe/CdMnSe or CdTe/CdMnTe) one can exploit the drastic differences in the Zeeman splitting occurring in different layers to pinpoint the localization in space of specific electronic states. If one (hole or electron) or both states involved in optical transition originate from SMS layer, this state will show very strong Zeeman splitting in the external magnetic field. Thus the SMS component can be used as a "marker" in order to bring out the general properties of wave function distribution.

Excitonic Zeeman splitting in nonmagnetic quantum well with SMS barriers can be applied to studies of the shape of interface profile and the influence of the growth conditions on the shape of the interface. If the interface is not completely flat, even a small fraction of magnetic atoms in the well close to the interface can significantly enhance the Zeeman exciton splitting in the quantum well. The sensitivity of this method allows one to detect the sharpness of an interface with one monolayer accuracy.

The MBE technique opens up possibilities to create hybrid structures with SMS useful for spintronic devices such as spin filters, spin transistors, tunneling magnetoresistance sensors. One of such possibilities is to fabricate hybrid metallic ferromagnetic-SMS structures. In such a case one can make use of the magnetic field exerted by the metallic ferromagnet positioned very close (on an atomic scale) to the SMS layer or quantum structure, thus affecting the spin splitting in the latter. One could use such a fringe fields to shape the band edges in such a fashion that an additional localization of the carriers in a two-dimensional of quantum well is induced leading to formation of quantum wires or dots.

The physics of SMS is currently a well-established part of solid state physics. In the investigations of bulk crystals and LD structures many problems are solved and new problems are waiting for further research. Particularly perspective seems to be investigation of layers and LD structures because of the broad technological possibilities and because the new important factor – dimensionality – and spin-dependent phenomena both can be intentionally regulated.

Acknowledgments

This paper was prepared on a basis of an invited talk presented in Latakia, Syria during Polish-Syrian Symposium held in May 2004. The author thanks the organizers for their fantastic hospitability.

REFERENCES:

1. Bauer G., Pascher H., Zawadzki W., (1992) in: Semicond. Sci. Technol., Vol. 7, page 703.

2. Dietl T., (1994) in: Handbook of Semiconductors, Vol. 3b, ed. Moss T.S., page 1251, Amsterdam: North-Holland.

3. Dietl T., (2002) in: Semicond. Sci. Technol., Vol. 17, page 377 (Special issue: Semiconductor Spintronics, guest ed. Hideo Ohno).

4. Furdyna J.K., (1991) in: Semimagnetic Semiconductors and Diluted Magnetic Semiconductors, eds. Averous M., Balkanski M., New York: Plenum.

5. Gałązka R.R., Kossut J., (1980) in: Lecture Notes in Physics, Vol. 133, ed. Zawadzki W., page 245, Springer Verlag, Berlin-Heidelberg-New York.

6. Gałązka R.R., Kossut J., (1982) in: Landolt-Börnstein New Series, Vol. lll/17b, eds. Madelung O., Schulz M., Weiss H., page 302, Springer Verlag, Berlin-Heidelberg-New York.

7. Gałązka R.R., Kossut J., Story T., (1999) in: Landolt-Börnstein New Series Vol. III/41b, ed. Rossler U., page 650, Springer Verlag, Berlin-Heidelberg-New York (Update to chapter 5, Vol. lll/17b).

8. Kossut J., Dobrowolski W., (1993) In: Handbook of Magnetic Materials, Vol. 7, ed. Buschow K.H.J., page 231, Amsterdam: North Holland.

9. Kossut J., Dobrowolski W., (1997) in: Narrow-Gap ll-VI Compounds for Optoelectronics and Electromagnetic Applications, ed. Capper P., page 401, Chapman and Hall, London.

10. Kossut J., (2001) in: Acta Phys. Pol. A, Vol. 100 (Supplement) page 111.

11. Ohno H., (2002) in: Japan Soc. Appl. Physics (JSAP International), No 5, page 4.

12. Semiconductors and Semimetals, (1988), Vol. 25, Diluted Magnetic Semiconductors, vol. eds. Furdyna J.K., Kossut J., Academic Press, San Diego.

13. Dobrowolski W., Kossut J., and Story T., (2003) in Buschow K.H.J. (ed.) Handbook of Magnetic Materials, II-VI Magnetic Semiconductors – New Bulk Materials and Low-Dimensional Quantum Structures, Vol. 15, page 289, Amsterdam: Elsevier North-Holland.

14. Story T., (2003) in: Monasreh M.O. (ed.) Optoelectronic properties of semiconductors and superlattices, Vol. 18, Khokhlov D. (ed.) Lead chalcogenides: physics and applications, chapter Semimagnetic semiconductors based on lead chalcogenides, page 385, Taylor and Francis Books Inc. New York, London.

15. Gałązka R.R., (in press) Encyclopedia of Modern Optics, Elsevier Science, London.

16. Mycielski J., (1981), Recent Develop. Condensed Matter Phys., Vol. 1, ed. Devreese J.T., Plenum Press, New York, page 725.